

# A Microwave and Quantum Chemical Study of (Trifluoromethyl)thiolacetic Acid, CF<sub>3</sub>COSH, a Compound with an Unusual Double-Minimum Potential

Harald Møllendal\*

Department of Chemistry, University of Oslo, Post Office Box 1033 Blindern, NO-0315 Oslo, Norway

Received: November 21, 2006; In Final Form: January 12, 2007

The microwave spectra of CF<sub>3</sub>COSH and one deuterated species, CF<sub>3</sub>COSD, have been investigated by Stark spectroscopy in the 40–80 GHz spectral range at –78 °C and by quantum chemical calculations using the HF, MP2, and B3LYP procedures with the aug-cc-pVTZ basis set. The microwave spectrum of one conformer was assigned. The conformations of the COSH and CF<sub>3</sub> groups determine the overall conformation of this rotamer. It was not possible experimentally to find precise values for the associated dihedral angles, but it appears that the COSH group is distorted somewhat from an exact synperiplanar arrangement, while the CF<sub>3</sub> group is rotated several degrees from a position where one of the C–F bonds eclipses the C–S bond. This rotamer tunnels through a transition state that has an exact C<sub>s</sub> symmetry, where one C–F bond eclipses the C–S bond and the COSH group is synperiplanar. Relative intensity measurements yielded 28(15) cm<sup>–1</sup> for the tunneling frequency. Two additional vibrationally excited states were assigned and their frequencies determined to be 94(30) and 184(40) cm<sup>–1</sup>, respectively. The theoretical calculations predict conflicting conformational properties for the identified rotamer. The B3LYP calculations find an exact synperiplanar arrangement for the COSH group, whereas the MP2 and HF calculations predict that this group is distorted slightly from this conformation. One of the C–F bonds is found to eclipse the C–S bond in the B3LYP calculations, while the MP2 calculations predict a slight deviation and the HF calculations a large deviation from the eclipsed position, as the corresponding F–C–C–S dihedral angle is calculated to be 0.9° (MP2) and 27.6° (HF). All three methods of calculations predict that a second rotamer coexists with the identified form but is several kJ/mol less stable. The spectrum of this form, which has overall C<sub>s</sub> symmetry and is predicted to have an antiperiplanar conformation for the COSH group with one of the C–F bonds eclipsing the C=O bond, was not identified.

## Introduction

There are relatively few reports of the structural and conformational properties of thiolacids (RCOSH). The prototype molecule, thiolformic acid (HCOSH), and several of its isotopologues have been studied extensively.<sup>1–5</sup> This compound was found to exist as a mixture of two planar rotameric forms. The O–C–S–H link of atoms is synperiplanar (sp) in the preferred form, which is 2.77(6) kJ/mol more stable than the antiperiplanar (ap) conformation. One rotamer was assigned for thiolacetic acid, CH<sub>3</sub>COSH. This form has a sp conformation for the said chain of atoms.<sup>6</sup>

Rotation about the C–C and C–S bonds may give rise to rotational isomerism in (trifluoromethyl)thiolacetic acid (CF<sub>3</sub>COSH), henceforth called TTA. Four typical isomers are depicted in Figure 1. Conformer I and II have a sp conformation for the thiolcarbonyl (COSH) group, whereas III and IV have an ap conformation for this group. The O3–C2–C1–F8 chain of atoms is ap in I and III and sp in II and IV. The S4–C2–C1–F8 link of atoms is sp in I and III and ap in II and IV.

TTA has been investigated by several experimental methods and quantum chemical calculations. Vapor density measurements showed that there is no association in the gaseous state, which is probably due to the absence of weak hydrogen

bonding.<sup>7</sup> Crowder<sup>8</sup> studied the gas, liquid, and solid states of TTA by infrared (IR) spectroscopy. He also investigated the Raman spectrum of the liquid.<sup>8</sup> A single C=O stretching vibration at 1755 cm<sup>–1</sup> was observed for the vapor, whereas two vibrational bands at 1739 and 1717 cm<sup>–1</sup> were present in the liquid state.<sup>8</sup> It was therefore suggested that there are two conformers in the liquid state but only one in the gas phase.<sup>8</sup> Crowder assumed that conformer III predominates in the gaseous state, because of intramolecular hydrogen bonding between the hydrogen atom of the thiol group and the nearest fluorine atom of the CF<sub>3</sub> group.<sup>8</sup>

An electron-diffraction and quantum chemical investigation was reported by Gobatto et al.<sup>9</sup> It was not possible in this electron-diffraction experiment to determine unambiguously the conformational properties of TTA.<sup>9</sup> They also undertook ab initio and density functional theory (DFT) calculations at five different levels of theory.<sup>9</sup> Interestingly, the conformational properties predicted from these calculations were found to vary significantly depending on the method used, making it impossible to draw definite conclusions from them.

This laboratory has had a long-standing interest in intramolecular hydrogen bonding, which has resulted in a number of recent investigations.<sup>10–22</sup> The thiol group is an interesting but relatively weak proton donor, often representing borderline cases of hydrogen bonding. However, a number of thiols displaying this interaction have been studied to date, including Z-3-mercapto-2-propenenitrile, HSCH=CHC≡N,<sup>23</sup> 3-butyne-1-thiol

\* To whom correspondence should be addressed. E-mail: harald.mollendal@kjemi.uio.no. Phone: +47 2285 5674. Fax: +47 2285 5441.

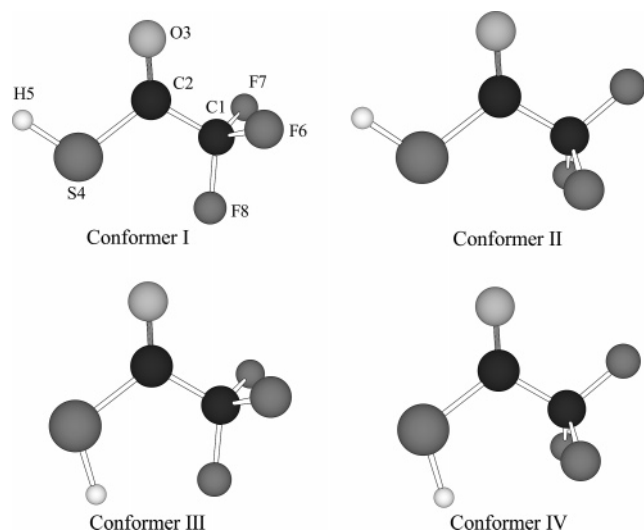


**Figure 1.** Four possible conformations of TTA. Conformers I and II have sp conformation for the thiolcarbonyl group, whereas III and IV have ap conformation for this group. The O3–C2–C1–F8 chain of atoms is ap in I and III and sp in II and IV. The S4–C2–C1–F8 link of atoms is sp in I and III and ap in II and IV. The four rotamers drawn here all have  $C_s$  symmetry. The MW spectrum of a rotamer similar to I, but with a significant deviation from  $C_s$  symmetry, was assigned in this work. The MW spectrum presents evidence that large-amplitude tunneling takes place in this conformer.

(HSCH<sub>2</sub>CH<sub>2</sub>C≡CH),<sup>11</sup> cyclopropanemethanethiol (C<sub>3</sub>H<sub>5</sub>CH<sub>2</sub>SH),<sup>24</sup> 2-furanmethanethiol (C<sub>4</sub>H<sub>3</sub>OCH<sub>2</sub>SH),<sup>25</sup> 1,2-ethanedithiol (HSCH<sub>2</sub>CH<sub>2</sub>SH),<sup>26</sup> 2-propenethiol (H<sub>2</sub>C=CHCH<sub>2</sub>SH),<sup>27</sup> aminoethanethiol (H<sub>2</sub>NCH<sub>2</sub>CH<sub>2</sub>SH),<sup>28–30</sup> methylthioglycolate (HSCH<sub>2</sub>COCH<sub>3</sub>),<sup>31</sup> thiiranemethanethiol (C<sub>2</sub>H<sub>3</sub>SCH<sub>2</sub>SH),<sup>32</sup> 3-butene-1-thiol (HSCH<sub>2</sub>CH<sub>2</sub>CH=CH<sub>2</sub>),<sup>33,34</sup> and 3-mercapto-propionitrile (HSCH<sub>2</sub>CHC≡N).<sup>35</sup>

The possibility that the thiol group might form an intramolecular hydrogen bond with one of the fluorine atoms as assumed by Crowder,<sup>8</sup> and the fact that no definite conclusions regarding the conformational properties of TTA had been derived in the previous electron-diffraction and quantum chemical study,<sup>8,9</sup> motivated us to undertake the present investigation.

The experimental method chosen was microwave (MW) spectroscopy because this method has an extreme accuracy and resolution, which is particularly advantageous in the study of molecules that present unusual structural or dynamical properties, which seemed to be the case for TTA.<sup>8,9</sup> The previous quantum chemical investigation<sup>9</sup> indicated that TTA represents a challenge for such calculations. It was therefore decided to perform quantum chemical calculations at much higher levels of theory than reported by Gobatto et al.<sup>9</sup> to augment the MW study. Fortunately, such high-level studies can now be performed conveniently, owing to the rapid advances in this field that has taken place in the decade since the work of Gobatto et al.<sup>9</sup>

## Experimental Section

A commercial sample of TTA was distilled before use. No impurities were seen in the MW spectrum, which was recorded in the 40–80 GHz spectral region using the Stark-modulated spectrometer of the University of Oslo, which measures the individual transitions with an estimated accuracy of ~0.10 MHz. Details of the construction and operation of this device, which has a 2-m Hewlett-Packard Stark cell, have been given elsewhere.<sup>13,36</sup> While recording the spectrum, the cell was cooled to dry ice temperature (–78 °C) to increase the intensity of the spectrum. Radio frequency microwave double-resonance experi-

ments (RFMWDR), similar to those performed by Wodarczyk and Wilson,<sup>37</sup> were also conducted to unambiguously assign particular transitions. The deuterated sample, CF<sub>3</sub>COSD, was prepared by admitting fumes of heavy water into the cell and then introducing the parent species. Roughly 50% deuteration was obtained in this manner.

## Results and Discussion

**Quantum Chemical Calculations.** A series of quantum chemical calculations were conducted on TTA, with the purpose of obtaining information for use in assigning the MW spectrum and investigating the structures of minima on the potential-energy hypersurface. All calculations were performed employing the Gaussian 03 suite of programs,<sup>38</sup> running on the 64 processor HP “superdome” computer in Oslo.

Gobatto et al.<sup>9</sup> performed self-consistent Hartree–Fock (HF) ab initio calculations on TTA at the HF/3-21G\* and HF/6-31G\* levels. They also took electron correlation into consideration using Møller–Plesset second-order perturbation calculations (MP2)<sup>39</sup> employing the 6-31G\* wave function (MP2/6-31G\* level). DFT calculations were also conducted<sup>9</sup> using both the local DFT approximation of Vosko, Wilk, and Nusair<sup>40</sup> (VWN) with a polarized triple-ζ basis set and VWN and nonlocal corrections of Becke (exchange)<sup>41</sup> and Perdew (correlation)<sup>42</sup> with a polarized triple-ζ basis set.

HF, MP2, and DFT calculations were also performed in the present case. Becke’s three-parameter hybrid functional<sup>43</sup> employing the Lee, Yang, and Parr correlation functional<sup>44</sup> (B3LYP) was employed in the DFT calculations. Dunning’s<sup>45</sup> correlation-consistent triple-ζ basis set, aug-cc-pVTZ, which includes polarized functions for the valence electrons and is augmented by additional diffuse functions, was used throughout this work.

Attempts to calculate the geometries of the four conformers sketched in Figure 1 were first made. The starting geometries were chosen to be close to those expected for these forms. Full geometry optimizations were carried out employing the default convergence criteria of Gaussian 03. The vibrational frequencies were calculated in each case, and no symmetry restrictions were imposed.

The HF, MP2, and B3LYP calculations all predict that conformers I and IV are minima on the potential-energy hypersurface (“stable” conformers) since only positive vibrational frequencies were calculated for each of them and conformer I was always found to be the global minimum. Subsequent B3LYP calculations found that II and III represent first-order transition states, since one imaginary vibrational frequency of 35.7i cm<sup>–1</sup> was calculated for II and one imaginary frequency of 26.0i cm<sup>–1</sup> was found for III. It is therefore concluded that conformers II and III are likely to be maxima on the potential-energy hypersurface and they are therefore not “stable” rotameric forms of TTA.

Conformer I presented a genuine problem for these calculations. The B3LYP method predicts that this rotamer has a symmetry plane ( $C_s$  symmetry) and two out-of-plane fluorine atoms. This finding contrasts the HF prediction, which yielded unusual values for the dihedral angles, exemplified by +27.6° for the F8–C1–C2–S4 dihedral angle and –4.3° for the O3–C2–S4–H5 dihedral angle, and consequently  $C_1$  symmetry for the equilibrium conformation of this conformer. The MP2 calculations did not predict an exact  $C_s$  symmetry but gave a small value of only 0.9° for the F8–C1–C2–S4 dihedral angle and –0.1° for the O3–C2–S4–H5 dihedral angle. The MP2 result is therefore in between the extremes represented by the

TABLE 1: HF, MP2, and B3LYP Geometries of Conformers I and IV of CF<sub>3</sub>COSH<sup>a</sup>

	HF		MP2		B3LYP	
	I	IV	I	IV	I	IV
Bond Length (pm)						
C1–C2	154.7	154.7	154.6	155.0	155.8	156.1
C1–F6	130.0	131.3	133.2	134.1	133.7	134.6
C1–F7	131.0	129.7	133.2	132.2	133.7	132.6
C1–F8	131.1	131.3	133.8	134.1	134.3	134.6
C2–O3	117.1	117.0	120.7	120.7	119.5	119.4
C2–S4	177.2	177.2	176.5	176.3	178.3	178.1
S4–H5	132.9	132.9	134.0	133.9	134.7	134.6
Angle (deg)						
C2–C1–F6	110.6	110.3	109.8	110.4	109.8	110.5
C2–C1–F7	109.1	110.7	109.8	110.8	109.8	110.7
C2–C1–F8	111.4	110.3	111.8	110.4	112.0	110.5
C1–C2–O3	120.1	120.6	119.8	121.0	119.9	120.9
C1–C2–S4	114.5	117.4	113.7	116.1	113.7	116.6
C2–S4–H5	93.8	98.1	91.7	96.1	92.6	97.3
Dihedral Angle (deg)						
F6–C1–C2–O3	33.2	120.4	60.5	120.7	59.7	120.4
F6–C1–C2–S4	–148.5	–59.6	–119.3	–59.3	–120.3	–59.6
F7–C1–C2–O3	–86.5	0.0	–58.9	0.2	–59.7	0.0
F7–C1–C2–S4	91.8	180.0	121.2	–179.8	120.3	180.0
F8–C1–C2–O3	154.1	–120.5	–179.2	–120.3	180.0	–120.4
F8–C1–C2–S4	–27.6	59.6	0.9	59.7	0.0	59.6
C1–C2–S4–H5	–173.8	0.0	179.8	0.1	180.0	0.0
O3–C2–S4–H5	4.3	180.0	–0.1	180.0	0.0	180.0

<sup>a</sup> The aug-cc-pVTZ basis set<sup>45</sup> has been used in these calculations; see text. Atom numbering is given on Figure 1.

results of the B3LYP and the HF calculations. The various structures that were calculated for conformer I are given in Table 1. The values of the uncorrected C1–C2 torsional fundamental found in the HF, MP2, and B3LYP calculations were 22.2, 11.9, and 14.6 cm<sup>–1</sup>, respectively. The remaining vibrational fundamentals calculated by the three methods (not given in Table 1) are all larger than about 200 cm<sup>–1</sup>.

The reason why the three quantum chemical methods yield quite different conformational results for this rotamer may perhaps be a result of a short nonbonded contact between S4 and F8. This distance is predicted to be 287 (HF), 278 (MP2), and 280 pm (B3LYP), which should be compared with Pauling's<sup>46</sup> sum, 320 pm, of the van der Waals radii of fluorine (135 pm) and sulfur (185 pm). The nonbonded distances are therefore 30–40 pm shorter than the sum of the van der Waals radii, a situation that appears to be difficult to handle consistently using the present levels of calculations. The fact that conflicting results are obtained in the HF, MP2, and B3LYP calculations with the aug-cc-pVTZ basis set implies that more elaborated calculations than the present ones are needed to determine accurately the geometry of conformer I by quantum chemical methods. Unfortunately, this could not be undertaken in this work, because of limitations on computational resources.

The less-stable conformer IV was predicted to have a symmetry plane (*C<sub>s</sub>* symmetry) regardless of the computational method that was used. The structures obtained for this rotamer are given in Table 1. The lowest vibrational frequency calculated for conformer IV is the C1–C2 torsional fundamental, whose uncorrected value was predicted to be 40.2 (HF), 32.9 (MP2), and 32.0 cm<sup>–1</sup> (B3LYP). The remaining vibrational fundamental frequencies were all predicted to be higher than about 200 cm<sup>–1</sup>.

There are some other interesting structural predictions in Table 1. The B3LYP bond lengths are found to be longer by 0.3–1.8 pm than their MP2 counterparts, with the exception of C2–O3 bond length, which is about 1 pm shorter. The HF bond lengths are generally, but not always, somewhat shorter than those found in the two other procedures, as expected. There is

good agreement between the angles, apart from those associated with the sulfur atom, where deviations of a few degrees are seen.

Additional results are given in Table 2, including the rotational constants,  $2P_{cc}$ , defined by  $2P_{cc} = I_a + I_b - I_c$  (where  $I_a$ ,  $I_b$ , and  $I_c$  are the principal moments of inertia), Watson's A-reduction centrifugal distortion constants,<sup>47</sup> the components of the dipole moment along the principal inertial axes, and the energy differences between the conformers corrected for zero-point vibrational effect and selected experimental parameters obtained for the ground (+) vibrational state. It is seen in this table that there are small differences between the rotational constants of conformers I and IV for calculations performed by the same procedure. The MP2 rotational constants are closer to their B3LYP counterparts and the experimental result for the (+) state than to the HF rotational constants. This is also true for the corresponding values of  $2P_{cc}$ .

Relatively large method-dependent variations are predicted for the corresponding values of  $\Delta_{JK}$ ,  $\Delta_K$ , and  $\delta_K$  centrifugal distortion constants, especially for conformer I. This is not surprising since the centrifugal distortion constants depend on the second derivative of the potential-energy hypersurface at the minimum formed by conformer I. This surface is rather different according to the computational procedure, as alluded to above.

All three methods predict that  $\mu_a$  is the largest component for conformer I, whereas  $\mu_b$  is largest component of conformer IV. The energy differences between II and I are calculated to be 0.7 (HF), 1.8 (MP2), and 2.5 kJ/mol (B3LYP), with conformer I as the more stable.

The unusual HF prediction of the structure of conformer I prompted further investigation into the nature of the torsion about the C1–C2 bond of this rotamer. HF/aug-cc-pVTZ calculations of energies were therefore performed for 10° intervals, from 0 to 180°, of the F8–C1–C2–S4 dihedral angle using the scan function of Gaussian 03 and allowing all remaining structural parameters to vary freely. The first

**TABLE 2: HF, MP2, and B3LYP Rotational Constants,  $2P_{cc}^a$ , Watson's A Reduction Centrifugal Distortion Constants and Energy Differences of Conformers I and IV of CF<sub>3</sub>COSH**

	HF		MP2		B3LYP		exptl <sup>d</sup>
	I	IV	I	IV	I	IV	I
Rotational Constants (MHz)							
A	3475.9	3473.9	3336.3	3329.6	3328.0	3328.3	3311.06(39)
B	1779.9	1775.5	1776.3	1776.9	1749.1	1743.3	1764.715(26)
C	1470.6	1467.2	1456.7	1456.1	1439.0	1435.8	1460.220(31)
Relation between Moments of Inertia <sup>a</sup> ( $10^{-20}$ u m <sup>2</sup> )							
$2P_{cc}^a$	85.64	85.67	89.06	89.12	89.60	89.75	92.916(29)
Centrifugal Distortion Constants (kHz)							
$\Delta_J$	0.172	0.155	0.161	0.167	0.167	0.171	2.5408(45)
$\Delta_{JK}$	5.83	1.42	22.9	1.88	14.7	1.80	19.129(16)
$\Delta_K$	-5.57	-1.18	-22.6	-2.13	-14.4	-1.55	e
$\delta_J$	0.0374	0.0335	0.0337	0.0370	0.0340	0.0367	-0.571(14)
$\delta_K$	-10.9	-3.42	-34.0	-5.05	-22.2	-4.17	e
Principal Inertial Axes Dipole Moment Components <sup>b</sup> ( $10^{-30}$ C m)							
$\mu_a$	6.1	2.5	7.0	3.2	6.6	3.1	f
$\mu_b$	3.0	7.6	4.0	8.2	3.1	7.1	f
$\mu_c$	0.0	0.0	0.0	0.0	0.0	0.0	f
Energy Difference <sup>c</sup> (kJ mol <sup>-1</sup> )							
$\Delta E$	0.0	0.7	0.0	1.8	0.0	2.5	f

<sup>a</sup>  $2P_{cc} = I_a + I_b - I_c$ , where  $I_a$ ,  $I_b$ , and  $I_c$  are the principal moments of inertia. Conversion factor  $505\,379.05\text{ MHz u }10^{-20}\text{ m}^2$ . <sup>b</sup> 1 Debye =  $3.3364 \times 10^{-30}\text{ C m}$ . The conformers have  $C_s$  symmetry. <sup>c</sup> Relative to conformer I. Electronic energy corrected for zero-point vibrational energy. These energies of conformer I were  $-2\,224\,287.90\text{ kJ/mol}$  (HF),  $-2\,228\,211.84\text{ kJ/mol}$  (MP2), and  $-2\,228\,210.05\text{ kJ/mol}$  (B3LYP). <sup>d</sup> Ground vibrational state, denoted the (+) state. <sup>e</sup> Not determined. Preset at zero in the least-squares fit; see text. <sup>f</sup> Not determined.

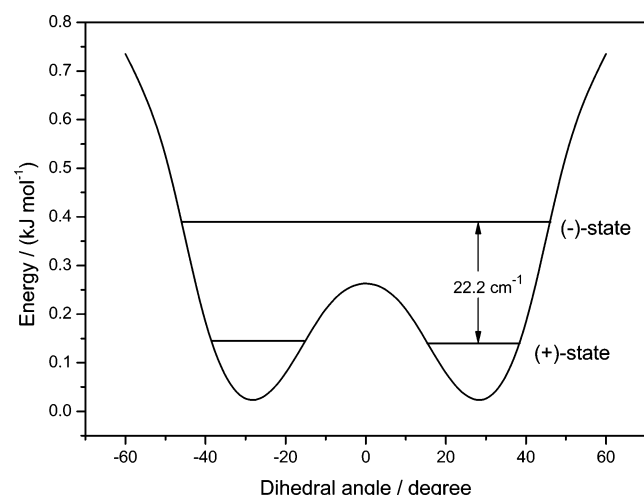


**Figure 2.** The HF/aug-cc-pVTZ potential function for rotation about the C1–C2 bond. The value of the F8–C1–C2–S4 dihedral angle is shown on the abscissa. The two lowest vibrational states, denoted the (+) and the (–) states, respectively, are indicated. This function repeats itself at every 120°. This potential function has maxima at 0° (0.24 kJ/mol relative to the minimum value) and  $\pm 59.6^\circ$  (0.71 kJ/mol) and minima at  $\pm 27.6^\circ$  (arbitrarily assigned the value 0 kJ/mol on this graph).

maximum of this function was calculated to occur when the F8–C1–C2–S4 dihedral angle is exactly 0° and the molecule has exact  $C_s$  symmetry. The barrier height is as small as 0.24 kJ/mol. A second maximum (0.71 kJ/mol above minimum) was found when the F8–C1–C2–S4 dihedral angle is  $\pm 59.6^\circ$ . This conformation is in fact conformer II (Figure 1). One imaginary vibrational frequency was calculated by the HF procedure for each of these two transition states. The values were  $17.9i\text{ cm}^{-1}$  for 0° and  $30.7i\text{ cm}^{-1}$  for  $\pm 59.6^\circ$  of the F8–C1–C2–S4 dihedral angle, respectively. The two maxima are therefore first-order saddle points.

A potential function shown in Figure 2 was now constructed using the available information for this rotamer. This function repeats itself for each 120°, owing to the symmetry of the

CF<sub>3</sub> group. The calculated harmonic frequency of  $22.2\text{ cm}^{-1}$  (the “tunneling frequency”) found for the minimum-energy conformer is indicated on this potential function. The lowest vibrational energy level is below the top of the barrier at 0°, while the second lowest vibrational energy level is above this barrier (Figure 2).

The HF and MP2 predictions indicate that there are two mirror images (enantiomers) of conformer I. Tunneling through the barrier at 0° transform the two enantiomers into one another. There is evidence for this kind of tunneling in the MW spectrum discussed below.

B3LYP/aug-cc-pVTZ calculations were finally undertaken for a rotation about the C2–S4 bond. The energy was calculated for each 10° of the O3–C2–S4–H5 dihedral angle and at the same time optimizing all remaining structural parameters by employing the scan function of Gaussian 03. Conformer I was seen to be transformed into conformer IV in this manner. The potential energy curve for this transformation is shown in Figure 3. The maximum, 39.6 kJ/mol, is found for a H5–S4–C2–O3 dihedral angle of 90°. There are no other minima but 0 and 180°. This result is supported partly by the HF and MP2 calculations above, where it was found that the O3–C2–S4–H5 dihedral angle is not exactly 0° but distorted slightly (Table 1).

**Strategy for Assigning the Microwave Spectrum.** The quantum chemical calculations above indicate that both conformers I and IV have relatively small rotational constants (Table 2), a low C1–C2 torsional frequency (less than  $50\text{ cm}^{-1}$ ), and about 5 other fundamental vibrations below  $500\text{ cm}^{-1}$  (not shown in Tables 1 and 2). All this means that the partition function of each of the two rotamers will be relatively large. Each quantum state will consequently have a relatively low population, resulting in comparatively weak MW transitions. It was therefore decided to investigate the molecule at dry ice temperature ( $-78^\circ\text{C}$ ) to reduce the size of the partition function, thereby obtaining the strongest possible spectrum with our instrumentation. It was also decided to investigate the spectrum in the upper frequency region (40–80 GHz) covered by our



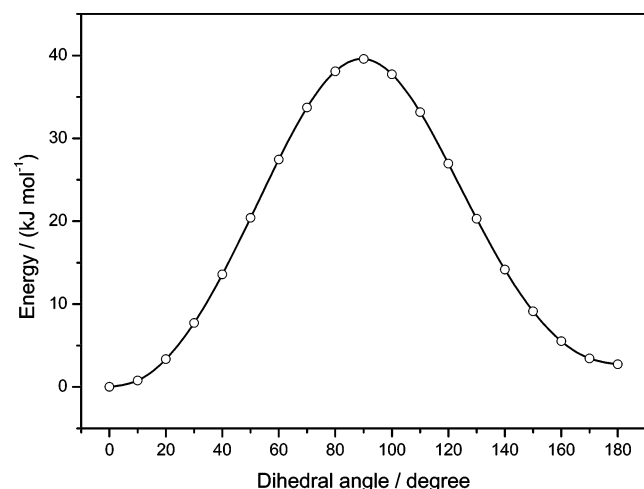


**Figure 3.** The B3LYP/avg-cc-pVTZ potential function for the rotation about the C2–S4 bond describing the transformation of conformer I into conformer IV. The O3–C1–C2–S4 dihedral angle shown on the abscissa takes the value 0° (0 kJ/mol) for conformer I and 180° (2.73 kJ/mol) for Conformer IV. This function has minima at 90° (39.6 kJ/mol).

spectrometer, because MW intensities are proportional to the square of the frequency and the strongest transitions are therefore found in this region.<sup>48</sup>

The low torsional frequency ( $<50\text{ cm}^{-1}$ ) indicates that several excited states of this fundamental should have rather high intensities relative to the intensities of the transitions of the ground vibrational state. The spectral patterns formed by these vibrationally excited states depend strongly on the potential function of the torsion. A near-harmonic potential, such as the one predicted in the B3LYP calculations, would lead to almost constant frequency spacing between successively excited states of a given MW transition. The intensities of the members of such a series would decrease steadily. Such a pattern was for example observed for the closely related molecule trifluoroacetic acid,  $\text{CF}_3\text{COOH}$ .<sup>49</sup>

On the other hand, a potential function with a double minimum, such as the one predicted in the HF calculations, would lead to a strikingly different pattern for the MW transitions of the vibrationally excited states. Two series of transitions, denoted the (+) state having the lower energy, and the (–) state having the higher energy, with almost equal intensities would exist in this case and be the strongest transitions of the spectrum. Further excited states of the torsion would in general not appear with a constant frequency spacing and a steadily diminishing intensity.

**Microwave Spectrum and Assignments.** The MW spectrum of TTA is very rich at  $-78\text{ }^\circ\text{C}$  with absorption lines occurring every few MHz throughout the entire MW region. Intervals separated by  $\sim 3.3\text{ GHz}$  had a higher density of transitions than elsewhere. The strongest lines of the spectrum were found in these pile-up regions. This pattern was expected for an  $^a\text{R}$  spectrum of TTA.

It is shown in Table 2 that the rotational constants predicted for conformers I and IV are very similar by coincidence. Both rotamers are predicted to have a component of the dipole moment along the a inertial axis. The observed pile-ups could therefore contain transitions originating from I and/or IV.

A detailed assignment of these pile-ups was achieved by scanning through these regions using a Stark field strength of about 50 V/cm. This field strength is sufficient to modulate the near-degenerate  $^a\text{R}$  transitions that have the highest values of the  $K_{-1}$  pseudo quantum numbers. A distinct feature seen for

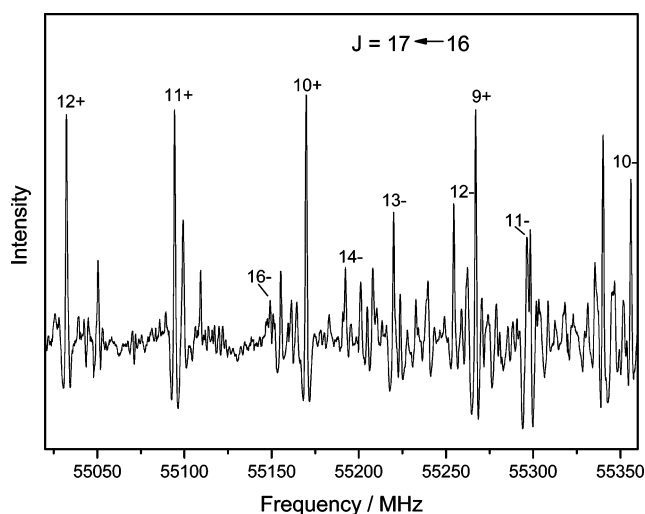


**Figure 4.** Microwave spectrum of TTA in the 55.0–55.4-GHz spectral interval showing a portion of the  $^a\text{R } J = 17-16$  transition region. The spectrum was taken using a Stark modulation field strength of about 50 V/cm<sup>-1</sup>. The numbers above the lines indicate the value of the  $K_{-1}$  coalescing line pair. The + sign denotes the (+) state, and the – sign denotes the (–) state caused by the double minimum potential (see text).

these pile-ups was two intense series of lines, which were used to obtain the first assignments. Transitions with corresponding values of  $K_{-1}$  of each series had similar intensities at  $-78\text{ }^\circ\text{C}$ . A portion of the spectrum illustrating this feature is shown in Figure 4. The two series with almost identical intensities are in accordance with the existence of a double minimum potential for the torsion about the C–C bond, as discussed in the previous paragraph. The strongest series is therefore called the (+) series and the less intense series is denoted the (–) series.

The assignments of several of the lines of both the (+) and the (–) series were confirmed by RFMWDR experiments.<sup>37</sup> Only  $^a\text{R}$  lines with  $J$  between 12 and 24 and with  $K_{-1} > 5$  were assigned, because the low- $K_{-1}$  transitions have very slow Stark effects and could not be modulated. b-Type lines were searched for but were not assigned unambiguously presumably because  $\mu_b$  is much less than  $\mu_a$  (Table 2) producing insufficient intensities for the b-type transitions. The fact that  $\mu_a$  is significantly larger than  $\mu_b$  is evidence that the assigned lines indeed belong to conformer I.

A total of 223  $^a\text{R}$  transitions of the (+) series and 217 transitions of the (–) series were fitted to Watson's A-reduction Hamiltonian using the I' representation,<sup>47</sup> using Sørensen's Rotfit program.<sup>50</sup> It was only possible to fit the rotational constants and three quartic centrifugal distortion constants ( $\Delta_J$ ,  $\Delta_{JK}$ , and  $\delta_J$ ). The two remaining quartic centrifugal distortion constants ( $\Delta_K$  and  $\delta_K$ ), which have very little influence on the frequencies of the  $^a\text{R}$  transitions assigned here, were preset at zero in the least-squares fit. The centrifugal distortion is remarkably large in this case, and it was necessary to include one sextic constant ( $\Phi_{KJ}$ ) to obtain a fit with a root-means square deviation comparable to the experimental uncertainty of  $\pm 0.10\text{ MHz}$ . The spectroscopic constants of the (+) and (–) states are shown in Table 3. The spectroscopic constants of the (+) state is also listed in Table 2 for convenient comparison with the theoretical values. The transitions used in the least-squares fits are listed in the Supporting Information, Tables 1S and 2S.

The root-mean-square deviations (Table 3) obtained for the two states (0.142 for the (+) and 0.204 MHz for the (–) state, respectively) are similar to the experimental uncertainty ( $\pm 0.10\text{ MHz}$ ), which is an indication that Watson's

**TABLE 3: Spectroscopic Constants<sup>a</sup> of the (+) and (−) States of CF<sub>3</sub>COSH and CF<sub>3</sub>COSD**

species	CF <sub>3</sub> COSH (+) state	CF <sub>3</sub> COSH (−) state	CF <sub>3</sub> COSD (+) state	CF <sub>3</sub> COSD (−) state
A (MHz)	3311.06(39)	3336.36(18)	3276.8(11)	3303.07(98)
B (MHz)	1764.715(26)	1764.046(19)	1717.021(68)	1716.245(88)
C (MHz)	1460.220(31)	1468.246(24)	1428.118(82)	1435.75(11)
Δ <sub>J</sub> (kHz)	2.5408(45)	0.5742(64)	1.9917(76)	0.695(11)
Δ <sub>JK</sub> (kHz)	19.129(16)	2.514(16)	16.155(29)	3.455(30)
δ <sub>J</sub> <sup>b</sup> (kHz)	−0.571(14)	−0.003(19)	−0.424(23)	−0.327(40)
Φ <sub>KJ</sub> <sup>c</sup> (Hz)	−4.839(23)	1.827(26)	−3.348(42)	1.137(48)
rms <sup>d</sup> (MHz)	0.142	0.204	0.144	0.206
no. transitions <sup>e</sup>	223	217	95	106
2P <sub>cc</sub> <sup>f</sup> (10 <sup>−20</sup> MHz u m <sup>2</sup> )	92.916(29)	93.759(16)	94.688(81)	95.475(86)

<sup>a</sup> A reduction I<sup>r</sup>-representation.<sup>47</sup> Uncertainties represent one standard deviation. <sup>b</sup> Further quartic constants preset at zero. <sup>c</sup> Further sextic constants preset at zero. <sup>d</sup> Root-mean-square deviation. <sup>e</sup> Number of transitions used in fit. <sup>f</sup> 2P<sub>cc</sub> = I<sub>a</sub> + I<sub>b</sub> − I<sub>c</sub>, where I<sub>a</sub>, I<sub>b</sub>, and I<sub>c</sub> are the principal moments of inertia. Conversion factor: 505 379.05 × 10<sup>−20</sup> MHz u m<sup>2</sup>.

Hamiltonian<sup>47</sup> is a sufficient approximation in this case. It is seen from Tables 2 and 3 that the MP2 and B3LYP calculations predict rotational constants for conformer I that are close to the experimental values. The centrifugal distortion constants are much larger for the (+) state than predicted in the theoretical calculations, whereas the centrifugal distortion constants of the (−) state are somewhat larger. This is not surprising, since the quantum chemical predictions are based on a harmonic model that is hardly expected to be accurate in this case.

The values of 2P<sub>cc</sub> = I<sub>a</sub> + I<sub>b</sub> − I<sub>c</sub> obtained for these two states, 92.916(29) and 93.759(16) × 10<sup>−20</sup> m<sup>2</sup> u (Table 3), respectively, are significantly larger than the calculated values shown in Table 2. They are also remarkably larger than the values found for trifluoroacetic acid, CF<sub>3</sub>COOH, (89.4736 × 10<sup>−20</sup> m<sup>2</sup> u),<sup>49</sup> its monodeuterated species, CF<sub>3</sub>COOD, (89.4832 × 10<sup>−20</sup> m<sup>2</sup> u),<sup>49</sup> and trifluoroacetaldehyde, CF<sub>3</sub>CHO, (89.32 × 10<sup>−20</sup> m<sup>2</sup> u).<sup>51</sup> These two compounds have C<sub>s</sub> symmetry and two out-of-plane fluorine atoms.

There could be several explanations for the increased values of 2P<sub>cc</sub> found for the title compound in comparison with those of trifluoroacetic acid and trifluoroacetaldehyde, such as changes in C–F bond lengths and CCF bond angles, or changes in the dihedral angles.

It was not possible to derive the dipole moment of this compound because none of the transitions observed displayed a resolved Stark effect. Relative intensity comparisons of the (+) and (−) states were made according to the procedure of Esbitt and Wilson,<sup>52</sup> assuming that μ<sub>a</sub> is the same for the two states. An energy difference corresponding to 28(15) cm<sup>−1</sup> was obtained in this manner, with the (+) state being lower in energy.

**Vibrationally Excited States.** Two additional vibrational excited states were assigned. They are denoted E1 and E2 in Table 4, where their spectroscopic constants are displayed. The transitions belonging to these two states have not been indicated on Figure 4. The transitions used to derive these parameters are listed in Tables 3S and 4S in the Supporting Information. Relative intensity measurements yielded 94(30) cm<sup>−1</sup> for E1 relative to the energy of the (+) state, whereas the E2 state is 184(40) cm<sup>−1</sup> higher in energy. There are large differences in the values of the centrifugal distortion constants as well as in the values of 2P<sub>cc</sub> (Table 4). Some of the transitions of the E1 state displayed partly resolved splittings. This state is therefore tentatively assigned as a successively excited state, presumably the third, of the C1–C2 torsion. The E2 state is perhaps an excited-state of a bending mode, because a frequency of about 200 cm<sup>−1</sup> is calculated for the lowest bending vibration in the HF, MP2, and B3LYP procedures. This excited-state has the lowest value found for 2P<sub>cc</sub>, and there was no indication of

**TABLE 4: Spectroscopic Constants<sup>a</sup> of Vibrationally Excited States of CF<sub>3</sub>COSH**

state	E1 <sup>b</sup>	E2 <sup>b</sup>
A (MHz)	3280.3(37)	3370.6(12)
B (MHz)	1759.76(19)	1764.592(78)
C (MHz)	1476.62(21)	1460.40(10)
Δ <sub>J</sub> (kHz)	0.171(22)	3.716(12)
Δ <sub>JK</sub> (kHz)	5.698(74)	30.584(93)
δ <sub>J</sub> <sup>c</sup> (kHz)	1.003(74)	−1.419(34)
Φ <sub>KJ</sub> <sup>d</sup> (Hz)	2.15(12)	0.24(20)
rms <sup>e</sup> (MHz)	0.272	0.190
no. transitions <sup>f</sup>	84	90
2P <sub>cc</sub> <sup>g</sup> (10 <sup>−20</sup> MHz u m <sup>2</sup> )	98.99(25)	90.281(85)

<sup>a</sup> A reduction I<sup>r</sup>-representation.<sup>47</sup> Uncertainties represent one standard deviation. <sup>b</sup> See text. <sup>c</sup> Further quartic constants preset at zero. <sup>d</sup> Further sextic constants preset at zero. <sup>e</sup> Root-mean-square deviation. <sup>f</sup> Number of transitions used in fit. <sup>g</sup> 2P<sub>cc</sub> = I<sub>a</sub> + I<sub>b</sub> − I<sub>c</sub>, where I<sub>a</sub>, I<sub>b</sub>, and I<sub>c</sub> are the principal moments of inertia. Conversion factor: 505 379.05 × 10<sup>−20</sup> MHz u m<sup>2</sup>.

**TABLE 5: Principal-Axis Coordinates of Conformers I and IV Obtained in the HF Calculations**

	I			IV		
	a	b	c	a	b	c
C1	−83.4	−12.6	−0.5	−83.9	−11.9	0.0
C2	53.1	60.3	−2.3	53.0	60.3	0.0
O3	57.1	177.3	−1.4	58.7	177.2	0.0
S4	193.9	−47.3	−0.7	198.4	−40.9	0.0
H5	281.1	52.3	11.4	138.7	−159.5	0.0
F6	−172.8	56.2	−65.1	−95.0	−88.2	106.2
F7	−122.7	−27.2	123.6	−181.1	73.9	0.0
F8	−74.7	−131.6	−54.9	−95.0	−88.2	−106.2

splittings. A decrease of this quantity compared to that of the ground vibrational state would be expected for a bending mode.

**Deuterated Species.** The assignment of the MW spectrum of the deuterated species, CF<sub>3</sub>COSD, was straightforward. The spectroscopic constants of the (+) and (−) states are shown in Table 3 and the spectra are listed in Tables 5S and 6S in the Supporting Information.

Interestingly, it is seen in Table 3 that the differences between the rotational constants of the (+) and (−) states of the parent species, CF<sub>3</sub>COSH, are close to the corresponding differences of the deuterated species, CF<sub>3</sub>COSD. If only the hydrogen atom took part in the tunneling process, these differences would have been much smaller for the deuterated species than for the parent species, because of the relatively large change in the reduced mass of this atom. If heavy atoms were involved in the tunneling, much smaller changes, such as those seen here, would be observed. The data in Table 3 therefore support the assumption that heavy atoms indeed take part in the tunneling.

It is noted that the values of  $2P_{cc}$  of both the (+) and (−) states increase significantly (Table 3) for the deuterated species compared with the counterparts of the parent species. If conformer I had  $C_s$  symmetry, the values of  $2P_{cc}$  would be expected to change only slightly, as was for example observed for trifluoroacetic acid ( $2P_{cc} = 89.4736$  for the parent and  $2P_{cc} = 89.4832 \times 10^{-20} \text{ m}^2 \text{ u}$  for the deuterated species, respectively; see above).

It is now possible to locate the position of the hydrogen atom (H5) using the rotational constants of the parent and deuterated species shown in Table 3 in Kraitchman's equations.<sup>53</sup> The values obtained in this manner are  $|a| = 264.8(6)$ ,  $|b| = 85.9(18)$ , and  $|c| = 96.4(16)$  pm using the rotational constants for the parent and deuterated species of the (+) state. The corresponding values obtained in case of the (−) state are  $|a| = 265.8(5)$ ,  $|b| = 83.3(17)$ , and  $|c| = 94.9(15)$  pm. The uncertainties in these Cartesian coordinates have been derived by propagating the uncertainties of the rotational constants. The uncertainties may be somewhat larger than the values shown here, owing to the large-amplitude vibration.

The values of the corresponding Cartesian coordinates are seen to be quite similar in the two cases, which is conclusive evidence that the (+) and (−) states belong to the same conformer and not to two different rotamers. The comparatively small variation between the two sets of coordinates is ascribed to be largely a result of the large-amplitude vibration.

The Cartesian coordinates obtained in the HF calculations for conformers I and IV are displayed in Table 5. The coordinates of the hydrogen atom in conformer I are  $|a| = 281.1$ ,  $|b| = 52.3$ , and  $|c| = 11.4$  pm. For conformer IV, a very different result of  $|a| = 138.7$ ,  $|b| = 159.5$ , and  $|c| = 0.0$  pm is predicted. The coordinates for conformer I, especially  $|a|$  and  $|b|$ , are in much better agreement with the experimental set of coordinates derived from the (+) and (−) states in the previous section, than the second set is. This is conclusive evidence that the assigned spectrum indeed belongs to conformer I and not to IV.

One problem remains. The  $c$  coordinate of the hydrogen atom calculated from Kraitchman's equations is rather large ( $|c| = 96.4(3)$  pm for the (+) state and  $|c| = 94.9(3)$  pm for the (−) state) compared to the HF result ( $|c| = 11.4$  pm). The large difference of more than 80 pm between the Kraitchman  $c$  coordinate (96.4 or 94.9 pm) and the HF counterpart (11.4 pm) is far too large to be explained by a large-amplitude vibration. It is in fact a strong indication that the thiolcarbonyl group is considerably more nonplanar than predicted in the HF calculations, where a dihedral angle of  $4.3^\circ$  was predicted for this chain of atoms (Table 1). However, it is not possible to say exactly how much the O3–C2–S4–H5 dihedral angle deviates from  $0^\circ$ , owing to the large-amplitude tunneling motion.

**Searches for Conformer IV.** All theoretical procedures predict that conformer IV should be somewhat less stable than I (Table 2). The largest dipole moment component of this rotamer is  $\mu_b$ , according to the calculations (Table 2). This dipole moment component is predicted to be somewhat larger than  $\mu_a$  for conformer I in the three quantum chemical procedures (Table 2). If this form were present in the same concentration as conformer I, it would have had a MW spectrum of comparable intensity to that of I. Extensive searches for b-type transitions of this rotamer have been performed, but no assignments could be made. There are, however, many unassigned lines remaining in the spectrum, so the existence of this species cannot be ruled out, but we think that there is significantly less of this rotamer than of conformer I, because

the majority of the strongest lines have been assigned to I. This finding is in accord with the theoretical predictions that conformer I is the more stable.

**Intramolecular Hydrogen Bonding.** It was suggested by Crowder<sup>8</sup> that conformer III is the preferred form of TTA, because this rotamer would be stabilized by a  $\text{H}\cdots\text{F}$  intramolecular hydrogen bond. The nonbonded distance between the hydrogen atom of the thiolcarbonyl group and the nearest fluorine atom of this rotamer is about 222 pm, according to the B3LYP calculations above, compared to 255 pm, which is the sum of the van der Waals radii of hydrogen (120 pm) and fluorine (135 pm).<sup>46</sup> The fact that the  $\text{H}\cdots\text{F}$  distance is shorter than the sum of the van der Waals radii by about 30 pm is obviously insufficient to make conformer III "stable". Instead, conformer III is found to be a transition state in the present theoretical calculations (see above).

The hydrogen atom of the thiolcarbonyl group would be bifurcated to the two fluorine atoms in conformer IV. However, the nonbonded B3LYP-distance between the fluorine atoms and the hydrogen atom is 265 pm, which is larger than 255 pm, the sum of the van der Waals radii.<sup>46</sup> Intramolecular hydrogen bonding would thus be a very minor effect in this rotamer.

There could be a hydrogen bond interaction between the hydrogen atom of the thiolcarbonyl group and the oxygen atom in conformer I. The nonbonded B3LYP distance between the two atoms is 258 pm compared to 260 pm, which is the sum of the van der Waals radii of hydrogen (120 pm) and oxygen (140 pm), which implies that there is only a very minor interaction in this case too.

## Conclusions

The MW spectrum of one rotamer of  $\text{CF}_3\text{COSH}$  has been assigned. This rotameric form is similar to conformer I (Figure 1) but distorted somewhat from  $C_s$  symmetry resulting in the existence of enantiomeric forms of this rotamer. The spectrum of the ground vibrational state is accompanied by several vibrationally excited states, whose irregular patterns indicate that tunneling between the two enantiomers occur, presumably through a transition state that has  $C_s$  symmetry. The tunneling frequency of the associated double minimum potential was determined to be  $28(15) \text{ cm}^{-1}$  by relative intensity measurements.

Quantum chemical calculations were performed using the aug-cc-pVTZ wave function<sup>45</sup> in HF, MP2, and B3LYP calculation procedures. The predictions for conformer I vary remarkably, since the HF and MP2 calculations predict  $C_1$  symmetry, whereas B3LYP calculations predict an exact  $C_s$  symmetry for conformer I. The HF and MP2 results imply that enantiomeric forms exist for this rotamer.

A potential function for rotation about the C1–C2 bond was calculated for conformer I using the HF procedure. This function (Figure 2) has a minimum when the S4–C2–C1–F8 dihedral angle is  $+27.6^\circ$  for one of the enantiomers (or  $-27.6^\circ$  for the other) and the C1–C2–S4–H5 dihedral angle is  $+4.3^\circ$  for this enantiomer (and  $-4.3^\circ$  for the other enantiomer). One maximum (0.24 kJ/mol above the minimum) is found at the exact sp conformation, where both the S4–C2–C1–F and C1–C2–S4–H5 dihedral angles are  $0^\circ$ . Other maxima (0.71 kJ/mol above the minimum) are found when the S4–C2–C1–F dihedral angle is  $+59.6^\circ$  or  $-59.6^\circ$ . It is not claimed that this potential function is accurate, but it seems to be in qualitative agreement with the observations.

The quantum chemical calculations predict that a second rotamer, denoted conformer IV (Figure 1), coexists with



conformer I but has a higher energy than I. The three methods of calculation predict that conformer IV has an ap conformer of the thiolcarbonyl group and one of the C–F bonds is eclipsing the C=O bond, resulting in an overall  $C_s$  symmetry. Conformer IV was not identified by MW spectroscopy.

Intramolecular hydrogen bonding does not seem to have much influence on the conformational properties of TTA.

**Acknowledgment.** We thank Anne Horn for her most helpful assistance. The Research Council of Norway (program for supercomputing) is thanked for a grant of computer time.

**Supporting Information Available:** MW spectra of TTA. This material is available free of charge via the Internet at <http://pubs.acs.org>.

## References and Notes

- Hocking, W. H.; Winnewisser, G. *J. Chem. Soc., Chem. Comm.* **1975**, 63.
- Hocking, W. H.; Winnewisser, G. *Z. Naturforsch. A* **1976**, 31A, 422.
- Hocking, W. H.; Winnewisser, G. *Z. Naturforsch. A* **1976**, 31A, 438.
- Hocking, W. H.; Winnewisser, G. *Z. Naturforsch. A* **1976**, 31A, 995.
- Hocking, W. H.; Winnewisser, G. *Z. Naturforsch. A* **1977**, 32A, 1108.
- Naito, T.; Ohashi, O.; Yamaguchi, I. *J. Mol. Spectrosc.* **1977**, 68, 32.
- Rochat, W. V.; Gard, G. L. *J. Org. Chem.* **1969**, 34, 4173.
- Crowder, G. A. *Appl. Spectrosc.* **1973**, 27, 440.
- Gobbato, K. I.; Della Vedova, C. O.; Mack, H.-G.; Oberhammer, H. *Inorg. Chem.* **1996**, 35, 6152.
- Møllendal, H.; Frank, D.; De, Meijere, A. *J. Phys. Chem. A* **2006**, 110, 6054.
- Cole, G. C.; Møllendal, H.; Guillemin, J.-C. *J. Phys. Chem. A* **2006**, 110, 9370.
- Cole, G. C.; Møllendal, H.; Guillemin, J.-C. *J. Phys. Chem. A* **2006**, 110, 2134.
- Møllendal, H.; Cole, G. C.; Guillemin, J.-C. *J. Phys. Chem. A* **2006**, 110, 921.
- Møllendal, H. *J. Phys. Chem. A* **2005**, 109, 9488.
- Askeland, E.; Møllendal, H.; Uggerud, E.; Guillemin, J.-C.; Moreno, J. R. A.; Demaison, J.; Huet, T. R. *J. Phys. Chem. A*, in press.
- Cole, G. C.; Møllendal, H.; Guillemin, J.-C. *J. Phys. Chem. A* **2005**, 109, 7134.
- Møllendal, H.; Samdal, S. *J. Phys. Chem. A* **2006**, 110, 2139.
- Petitprez, D.; Demaison, J.; Włodarczak, G.; Guillemin, J.-C.; Møllendal, H. *J. Phys. Chem. A* **2004**, 108, 1403.
- Lovas, F. J.; Suenram, R. D.; Plusquellic, D. F.; Møllendal, H. *J. Mol. Spectrosc.* **2003**, 222, 263.
- Samdal, S.; Møllendal, H. *J. Phys. Chem. A* **2003**, 107, 8845.
- Møllendal, H.; Kozhushkov, S. I.; de Meijere, A. *Asian Chem. Lett.* **2003**, 7, 61.
- Møllendal, H. *NATO ASI Ser., Ser. C* **1993**, 410, 277.
- Cole, G. C.; Møllendal, H.; Guillemin, J. C. *J. Phys. Chem. A* **2007**, 111, 1259.
- Marstokk, K.-M.; Møllendal, H. *Acta Chem. Scand.* **1991**, 45, 354.
- Marstokk, K.-M.; Møllendal, H. *Acta Chem. Scand.* **1994**, 48, 298.
- Marstokk, K.-M.; Møllendal, H. *Acta Chem. Scand.* **1997**, 51, 653.
- Bhaumik, A.; Brooks, W. V. F.; Dass, S. C.; Sastry, K. V. L. N. *Can. J. Chem.* **1970**, 48, 2949.
- Barkowski, S. L.; Hedberg, K. *J. Am. Chem. Soc.* **1987**, 109, 6989.
- Nandi, R. N.; Boland, M. F.; Harmony, M. D. *J. Mol. Spectrosc.* **1982**, 92, 419.
- Caminati, W.; Velino, B.; Schäfer, L.; Ewbank, J. D.; Siam, K. *J. Mol. Struct.* **1989**, 197, 123.
- Fantoni, A. C.; Caminati, W. *J. Mol. Spectrosc.* **1990**, 143, 389.
- Marstokk, K.-M.; Møllendal, H.; Stenstrøm, Y. *Acta Chem. Scand.* **1994**, 48, 711.
- Marstokk, K.-M.; Møllendal, H. *Acta Chem. Scand., Ser. A* **1986**, A40, 402.
- Marstokk, K.-M.; Møllendal, H. *NATO ASI Ser., Ser. C* **1987**, 212, 57.
- Marstokk, K.-M.; Møllendal, H. *Acta Chem. Scand., Ser. A* **1983**, A37, 477.
- Møllendal, H.; Leonov, A.; de Meijere, A. *J. Phys. Chem. A* **2005**, 109, 6344.
- Wodarczyk, F. J.; Wilson, E. B., Jr. *J. Mol. Spectrosc.* **1971**, 37, 445.
- Frisch, M. J.; Trucks, G. W.; Schlegel, H. B.; Scuseria, G. E.; Robb, M. A.; Cheeseman, J. R.; Montgomery, J. A., Jr.; Vreven, T.; Kudin, K. N.; Burant, J. C.; Millam, J. M.; Iyengar, S. S.; Tomasi, J.; Barone, V.; Mennucci, B.; Cossi, M.; Scalmani, G.; Rega, N.; Petersson, G. A.; Nakatsuji, H.; Hada, M.; Ehara, M.; Toyota, K.; Fukuda, R.; Hasegawa, J.; Ishida, M.; Nakajima, T.; Honda, Y.; Kitao, O.; Nakai, H.; Klene, M.; Li, X.; Knox, J. E.; Hratchian, H. P.; Cross, J. B.; Adamo, C.; Jaramillo, J.; Gomperts, R.; Stratmann, R. E.; Yazyev, O.; Austin, A. J.; Cammi, R.; Pomelli, C.; Ochterski, J. W.; Ayala, P. Y.; Morokuma, K.; Voth, G. A.; Salvador, P.; Dannenberg, J. J.; Zakrzewski, V. G.; Dapprich, S.; Daniels, A. D.; Strain, M. C.; Farkas, O.; Malick, D. K.; Rabuck, A. D.; Raghavachari, K.; Foresman, J. B.; Ortiz, J. V.; Cui, Q.; Baboul, A. G.; Clifford, S.; Cioslowski, J.; Stefanov, B. B.; Liu, G.; Liashenko, A.; Piskorz, P.; Komaromi, I.; Martin, R. L.; Fox, D. J.; Keith, T.; Al-Laham, M. A.; Peng, C. Y.; Nanayakkara, A.; Challacombe, M.; Gill, P. M. W.; Johnson, B.; Chen, W.; Wong, M. W.; Gonzalez, C.; Pople, J. A. *Gaussian 03*, revision B.03; Gaussian, Inc.: Pittsburgh PA, 2003.
- Møller, C.; Plesset, M. S. *Phys. Rev.* **1934**, 46, 618.
- Vosko, S. H.; Wilk, L.; Nusair, M. *Can. J. Phys.* **1980**, 58, 1200.
- Becke, A. D. *Phys. Rev. A* **1988**, 38, 3098.
- Perdew, J. P. *Phys. Rev. B* **1986**, 33, 8822.
- Becke, A. D. *J. Chem. Phys.* **1993**, 98, 5648.
- Lee, C.; Yang, W.; Parr, R. G. *Phys. Rev. B* **1988**, 37, 785.
- Dunning, T. H., Jr. *J. Chem. Phys.* **1989**, 90, 1007.
- Pauling, L. *The Nature of the Chemical Bond*; Cornell University Press: New York, 1960.
- Watson, J. K. G. *Vibrational Spectra and Structure*; Elsevier: Amsterdam, 1977; Vol. 6.
- Gordy, W.; Cook, R. L. *Techniques of Chemistry, Vol. XVII: Microwave Molecular Spectra*; John Wiley & Sons: New York, 1984; Vol. XVII.
- Stolwijk, V. M.; Van, Eijck, B. P. *J. Mol. Spectrosc.* **1985**, 113, 196.
- Sørensen, G. O. ROTFIT. Personal communication, 1972.
- Woods, R. C.; Wilson, E. B. *J. Chem. Phys.* **1967**, 46, 4789.
- Esbit, A. S.; Wilson, E. B. *Rev. Sci. Instrum.* **1963**, 34, 901.
- Kraitchman, J. *Am. J. Phys.* **1953**, 21, 17.